Microchimica Acta (2019) 186: 265
https://doi.org/10.1007/s00604-019-3377-x

ORIGINAL PAPER

Enzyme-free electrocatalytic sensing of hydrogen peroxide using a glassy carbon electrode modified with cobalt nanoparticle-decorated tungsten carbide

Muthaiah Annalakshmi[1] · Paramasivam Balasubramanian[1] · Shen-Ming Chen[1] · Tse-Wei Chen[1,2]

Received: 26 December 2018 / Accepted: 21 March 2019 / Published online: 30 March 2019

Abstract

An efficient non-enzymatic electrochemical sensor for hydrogen peroxide (H_2O_2) was constructed by modifying a glassy carbon electrode (GCE) with a nanocomposite prepared from cobalt nanoparticle (CoNP) and tungsten carbide (WC). The nanocomposite was prepared at low temperature through a simple technique. Its crystal structure, surface morphology and elemental composition were investigated via X-ray diffraction, transmission electron microscopy and X-ray photoelectron spectroscopy. The results showed the composite to be uniformly distributed and that the CoNP are well attached to the surface of the flake-like WC. Electrochemical studies show that the modified GCE has an improved electrocatalytic activity toward the reduction of H_2O_2. H_2O_2 can be selectively detected, best at a working voltage of −0.4 V (vs. Ag/AgCl), with a 6.3 nM detection limit over the wide linear range from 50 nM to 1.0 mM. This surpasses previously reported non-enzymatic H_2O_2 sensors. The sensor was successfully applied to the determination of H_2O_2 in contact lens solutions and in spiked serum samples.

Keywords Reactive oxygen species (ROS) · Non-enzymatic · Electrochemical sensor · Metal carbides · Metal nanoparticle

Introduction

Hydrogen peroxide (H_2O_2) is a crucial mediator and a significant reducing/oxidizing agent in various biological and chemical reactions [1]. This is due to its antioxidant property, easy storage, microbial control and high availability, and its use in numerous fields [2, 3]. H_2O_2 is a representative of reactive oxygen species (ROS), products of in-vivo metabolism and also a byproduct of most oxidase enzymes, which can diffuse through the cell membranes freely [4]. H_2O_2 play a vital role in tumor incidence and also in physiological pathways, migration, immune system function and cell growth, and thus cause various human disorder such as cancer, Alzheimer's disease, atherosclerosis, myocardial infraction, DNA damage and Parkinson's disease etc., [5, 6]. Hence, exploring the rapid, sensitive, selective, low-cost and reliable analytical method for the quantification of H_2O_2 is significant in biological environments. Several analytical protocols have been developed for H_2O_2 assay, such as fluorescence [7], chromatography [8], spectrometry [9], chemiluminescence [10] and electrochemical methods [11–13]. The electrochemical method is the most promising method due to their intrinsic features such as low cost, high sensitivity, selectivity, rapidity and real time monitoring ability toward the H_2O_2 determination [14]. The enormous studies have been made on the materials with excellent electrocatalysis for non-enzymatic H_2O_2 electrochemical sensors such as noble metal nanoparticles [15], carbon materials [16], metal oxides [17].

Transition metal carbides (TMCs) has been significantly used as a superior electrocatalysts in many electrochemical devices such as supercapacitors [18], photochemical setup and electrochemical methods [19] and oxygen reduction reaction (ORR) for fuel cells [20] due to the outstanding electrical conductivity and chemical stability. Thus, TMCs are evolving as auspicious and attractive electrode materials for

Electronic supplementary material The online version of this article (https://doi.org/10.1007/s00604-019-3377-x) contains supplementary material, which is available to authorized users.

✉ Shen-Ming Chen
smchen78@ms15.hinet.net

[1] Department of Chemical Engineering and Biotechnology, National Taipei University of Technology, Taipei 106, Taiwan, Republic of China

[2] Research and Development Center for Smart Textile Technology, National Taipei University of Technology, No.1, Section 3, Zhongxiao East Road, Taipei 106, Taiwan, Republic of China

electrochemical applications. For example, cobalt carbide (Co_2C) was reported as a superior electrocatalysts for the hydrogen evolution reaction (HER) from water splitting [21]. Fan et al., developed the Fe-doped Ni_3C nanosheets exhibited outstanding electrocatalytic performance in both O_2 evolution reaction (OER) and HER [22]. Meyer et al., fabricated the transition metal carbides including WC, Mo_2C, TaC and NbC were used as a proficient electrocatalysts in HER [23]. It can be concluded that TMCs has significantly improved electrocatalytic behaviour towards the detection of H_2O_2 than that of metal oxides, alloys and carbon materials.

Tungsten carbide (WC) is one potential nanocatalyst and has received specific interest in electrocatalysts, due to its sufficient ionic conductivity, earth abundant, and low-toxicity [24]. Many reports are developed on the tungsten carbide (WC) as an electrocatalyst based on the several electrochemical applications such as WC/carbon composite for HER [25], WC NP for HER [26], WC/graphene for HER [27]. Encapsulation of metal carbides within metal nanoparticles, oxides or carbon materials has been proposed as an effective strategy to further improving the catalytic activity of WC. The improved electrochemical activity is ascribed to the alteration of the surface structures and electronic properties of the metal carbides or active metal species [28]. The doping of VIII group metals are feasible due to the electron rich capacity can effectively decrease the unoccupied d-orbitals of metals of carbides [29]. The incorporating of metal (Fe, Ni, Co, Cu) on metal carbides has been enhanced the catalytic activity. Among them, metallic Co has possessed tremendous catalytic properties, various literature reported on Co incorporated to metal carbides [29, 30]. To the best of our knowledge, no literature available on the fabrication of Co doped WC and its electrochemical sensing application towards H_2O_2.

We report here on the preparation of Co NP decorated WC (WCC) through a simple and low temperature method. Further, WCC was applied as an electrode modifier to create a novel, highly sensitive and selective non-enzymatic H_2O_2 sensor. The electrocatalytic studies shows that WCC modified glassy carbon electrode (GCE) exhibited an excellent electrochemical performance with a wide linear range and low limit of detection. The sensor was applied to practical application in contact lens solution and blood serum samples. The synthesis of WCC and electrochemical detection of H_2O_2 is shown in Scheme. 1.

Experimental section

Materials and methods

Disodium hydrogen phosphate (Na_2HPO_4), sodium dihydrogen phosphate (NaH_2PO_4), cobalt nitrate hexahydrate ($Co(NO_3)_2.6H_2O$), sodium borohydride ($NaBH_4$), hexacarbonyl tungsten ($W(CO)_6$), ethylene glycol (EG) and oleylamine (70%) were purchased from Sigma-Aldrich (https://www.sigmaaldrich.com/catalog/product). All commercial chemicals and reagents were of analytical grade without further purification. For the purpose of electrochemical experiments, 0.05 M phosphate buffer used as supporting electrolyte, prepared by mixing Na_2HPO_4 and NaH_2PO_4. The deionized water (DIW) was used to prepare the all required solutions.

The surface morphology and the formation of WC-Co nanocomposite were investigated by transmission electron microscopy (TEM, JEOL 2100F) under an accelerating voltage of 200 kV. The crystal structure of WCC NPs was scrutinized by using X-ray diffraction studies (XRD, XPERT-3 diffract meter with Cu-Kα; K = 1.54 Å). The electronic state of Co, W and C in WCC were confirmed by using X-ray photoelectron spectroscopy (XPS) was performed in Thermo scientific multilab 2000. The interfacial electrocatalytic behaviour of the modified electrode was investigated by Electrochemical impedance spectroscopy (EIS, IM6ex ZAHNER impedance measurement system) at a potential of 0.2 V (AC potential: 5 mV) within a frequency range of 0.01 to 100 kHz. The electrochemical sensing performances of WCC modified electrode toward H_2O_2 detection, were investigated by cyclic voltammetry (CV) and amperometry techniques in CHI 1205C electrochemical analyzer (CH Instruments Company, made in the U.S.A). The conventional three-electrode system were used such as a saturated Ag/AgCl/Sat. KCl as a reference electrode, a glassy carbon electrode (GCE area: 0.071 cm^2 and rotating disk electrode (RDE) area: 0.2 cm^2 (rpm = 1400)) as a working electrode and a platinum wire used as an auxiliary electrode.

Synthesis of the cobalt nanoparticle-decorated tungsten carbide (WCC) nanocomposite

To synthesis the WC nanoparticle, a mixture of EG (10 mL) and oleylamine (5 mL) were degassed with N_2 gas for 5 min at room temperature in a three-neck flask. Then, 250 mg $W(CO)_6$ was added to the mixture of EG and oleylamine and the reaction mixture was vigorously stirred for 2 h at 100 °C under N_2 atm. Then the solution was allowed to cool at room temperature. Then the solution was centrifuged and washed several times with water and ethanol and dried in vacuum oven at 80 °C for 12 h. To receive WC, the crude product was carbonized at 800 °C for 2 h under N_2 flow. Next, 0.1 g WC flakes was dispersed in 20 mL of DIW and 50 mg $Co(NO_3)_2.6H_2O$ was added into the WC dispersion under ultrasonication. Then, 5 mL freshly prepared 0.1 M $NaBH_4$ solution were mixed together and ultrasonicated at 60 °C for 2 h. The resultant

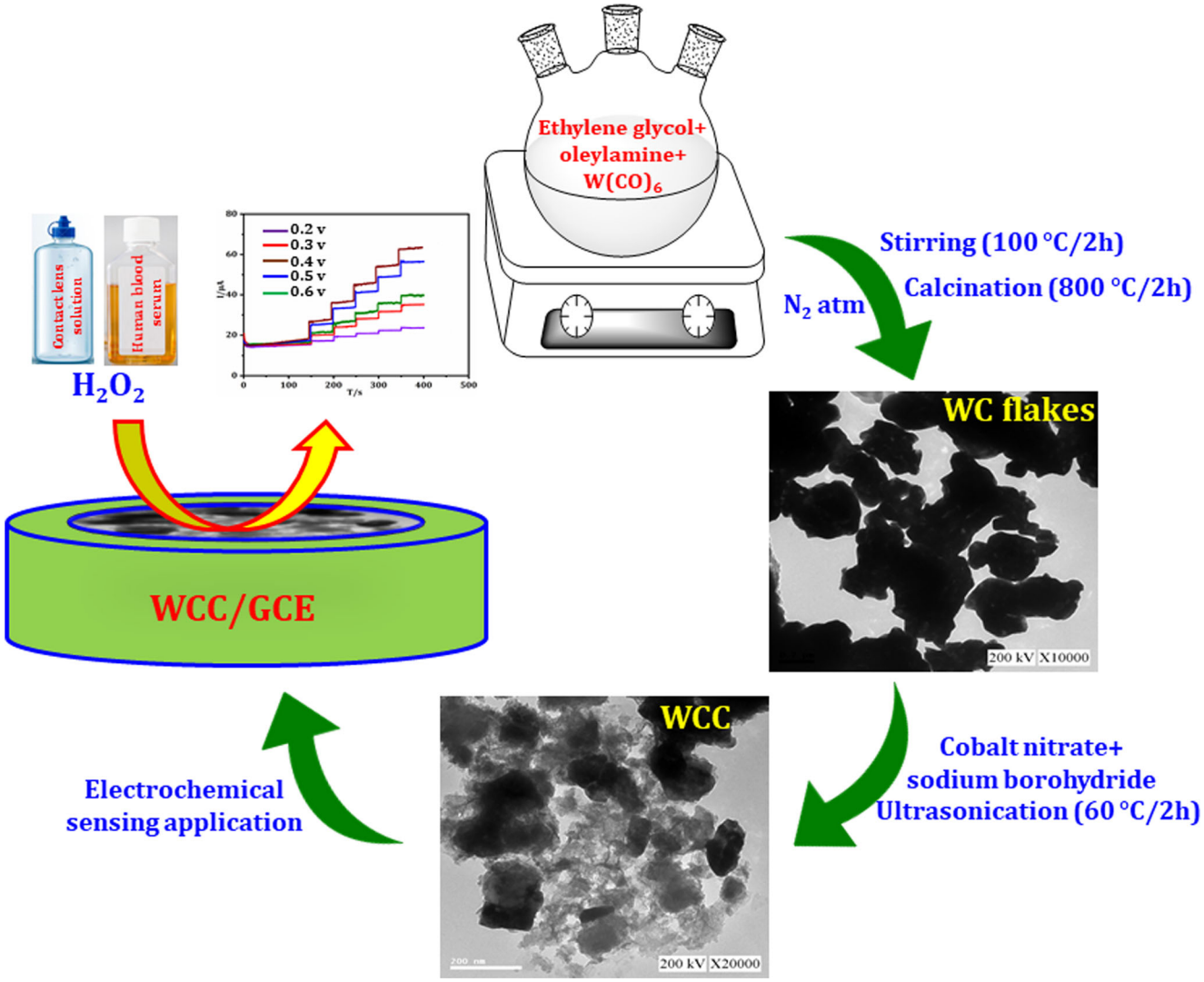

Scheme 1 Pictorial representation of the synthesis of cobalt nanoparticle-decorated tungsten carbide (WCC) and its H_2O_2 sensing application

solution was centrifuged and washed with ethanol and water then transferred to vacuum oven for drying at 80 °C. Finally, the desired WCC nanoparticle was prepared and it was used for the further applications.

Fabrication of WCC modified electrode

For the electrode fabrication process, the synthesized WCC (2 mg) was dispersed in 1 mL DIW and sonicated for 30 min. In before, the glassy carbon electrode (GCE) was polished by 0.05 mm alumina powder and washed with DIW and 6 μL of WCC dispersion was drop-cast onto the surface of pre-cleaned GCE, dried in a hot air oven. Subsequently, to remove the unbounded materials on GCE were washed with DIW and then the fabricated electrode was used to the determination of H_2O_2. All the electrochemical experiments were carried out in deoxygenated buffer.

Results and discussion

Choice of material

Transition metal carbides (TMCs) has been significantly used as a superior electrocatalysts in many electrochemical devices such as supercapacitors [18], photochemical setup and electrochemical methods [19] and oxygen reduction reaction (ORR) for fuel cells [20] due to the outstanding electrical conductivity and chemical stability. Encapsulation of metal carbides within metal nanoparticles, oxides or carbon materials has been proposed as an effective strategy to further improving the catalytic activity of WC. The improved electrochemical activity is ascribed to the alteration of the surface structures and electronic properties of the metal carbides or active metal species [28]. The incorporating of metal (Fe, Ni, Co, Cu) on metal carbides has been enhanced the

catalytic activity. Among them, metallic Co has possessed tremendous catalytic properties, various literature reported on Co incorporated to metal carbides [29, 30]. To the best of our knowledge, no literature available on the fabrication of Co decorated WC and its electrochemical sensing application towards H_2O_2. Hence, we have synthesized the Co nanoparticle decorated WCC and it was successfully employed as an excellent electrocatalyst for the detection of H_2O_2.

Surface characterization

The morphology of the WC and WCC was characterized by transmission electron microscopy (TEM). From Fig. 1a exhibits TEM image of WC, the WC appears as flake-like structure with the average particle size is to be around 500 nm. Further, the observed TEM image (Fig. 1b) of WCC, indicates that the cobalt nanoparticles are embedded on the surface of WC flakes and it confirms the formation of WCC. The selective area electron diffraction (SAED) (inset of Fig. 1b) patterns also validated the formation of WCC. Further, the corresponding elemental mapping images (Fig. 1c (mix), D (W), E (Co), F (C)) confirmed the uniform distribution and presence of W, Co and C in WCC.

The crystal structure of WC and WCC have been investigated by X-ray diffraction (XRD) studies (Fig. 2a). The XRD spectrum of WC (red) shows the diffraction peaks at 31.5° (001), 35.6° (100), 48.3° (101), 64° (110), 65.7° (002), 73.1° (111), 75.5° (200), 77.12° (102), and 84° (201) are consistent with the diffraction planes of hexagonal WC (diamond; JCPDS 073–0471). For the XRD spectra of WCC (green), the diffraction peaks appeared at 44.1° (111) and 51.6° (002) (star; JCPDS 15–0806) with the standard diffraction peaks of WC, which results validates that the surface decoration of Co NP on WC flakes.

The elemental composition and electronic state of W, C and Co in WCC was investigated via X-ray photoelectron spectroscopy (XPS). The characteristics survey spectrum (Fig. 2b) indicate the existence of W, C and Co in WCC. The high resolution XPS spectrum of W (Fig. 2c) displays two major signal, W $4f_{7/2}$ and W $4f_{5/2}$ at 33.8 and 36.0 eV respectively, confirms the formation of WC. In addition, the two less intense peaks appeared around 37.6 (W $4f_{7/2}$) and 39.8 eV (W $4f_{5/2}$), which are assigned to W 4f orbits of surface WO_x passivation layer [31]. On the other hand, the Gaussian fitting peaks of Co 2p (Fig. 2d) exhibits two main peaks at binding energies of 784.3 and 799.7 eV of Co (II), corresponding to Co $2p_{3/2}$ and Co $2p_{1/2}$, respectively. Further, the high energy side of core level binding energies were appeared due to the high spin state of Co (II), while the low spin Co (III) does not show any satellite peaks [32]. It can be concluded that the oxidation state of Co nanoparticles in WCC is +2 [33].

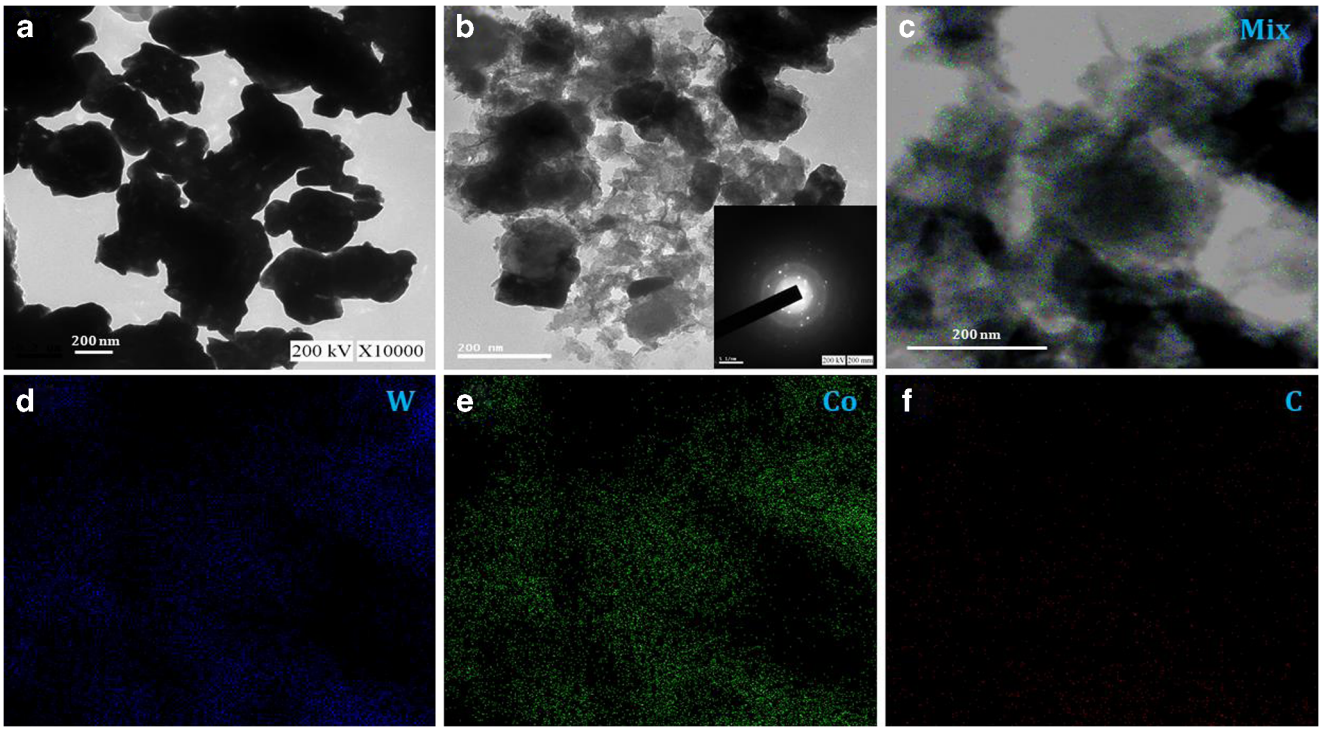

Fig. 1 TEM image of WC (**a**) and WCC (inset SAED pattern) (**b**). Elemental mapping of WCC; Mix (**c**), W (**d**), Co (**e**), and C (**f**)

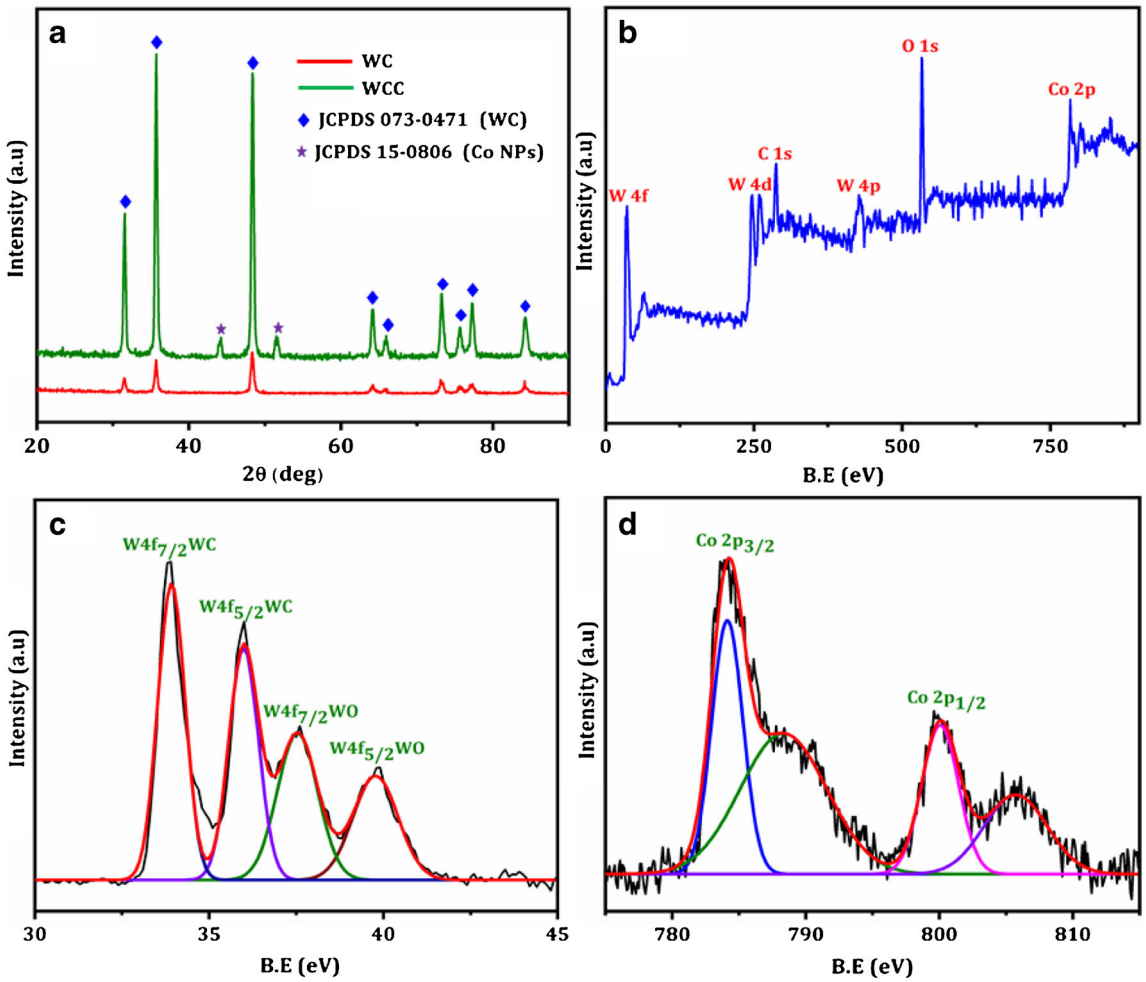

Fig. 2 XRD of WC (red) and WCC (green) (**a**), XPS survey spectrum of WCC (**b**), W4f (**c**), and Co 2p (**d**)

Electrocatalytic properties of different modified electrodes

In Electrochemical impedance spectroscopy (EIS) (Fig. 3a), a semicircle at high frequencies and linear part at low frequencies represent to the electron transfer limited process and diffusion process, respectively. Typically, the charge transfers resistance (R_{ct}) can be defined by the diameter of the semicircle part, its value varies when different substances are adsorbed on to the surface of electrode. As depicted in Fig. 3a, the calculated charge transfer resistance (R_{ct}) of unmodified GCE (curve a) is about 344 Ω. After introducing WC on the surface of GCE, the R_{ct} value was decreased (R_{ct} = 30 Ω, curve b) due to the good ionic conductivity. An anticipated, the minimal resistance value (R_{ct} = 6 Ω, curve c) was obtained at WCC/GCE in compared with that of bare GCE and WC/GCE, promote a rapid electron transfer between the electroactive material and electrolyte. These results indicate the enhanced electrocatalytic activity of WC has been significantly enhanced by introducing Co NP and WCC provides essential pathways for the development of H_2O_2 detection.

Figure 3b exhibits the CVs of bare GCE, WC/GCE, and WCC/GCE, and in the absence and presence of 1 mM H_2O_2 in 0.05 M phosphate buffer (pH 7) at a scan rate of 50 mV s^{-1}. As can be seen from Fig. 3b, in the case of bare GCE (curve a), WC/GCE (curve b), Co NP (curve c) and WCC (curve d), no characteristic peaks were appeared without the addition of H_2O_2, which clearly explains that the electrodes are inactive at this potential window. In the case of bare GCE (curve a'), only displays a very less reduction peak current (I_{pc}: 1.3 μA) while adding the 1 mM H_2O_2 due to the less electrocatalytic activity toward the reduction of H_2O_2. Besides, WC/GCE (curve b') (I_{pc}: 2.9 μA) and Co NP (curve c') (I_{pc}: 3.7 μA) showed obviously increased catalytic reduction current for 1 mM H_2O_2 when compared with the bare GCE. Interestingly, addition of 1 mM H_2O_2 caused in an enhanced cathodic peak current (I_{pc}: 6.7 μA) at lower reduction potential (E_{pc}: −0.4 V) on the WCC/GCE (curve c') electrode matrix. These results revealed that the modified WCC effectively promoted the electron transfer between the electrolyte and the electrode surface. Many possible descriptions may contribute to these remarks: (i) flakes-like structure of WC and nanosheets-like structure Co NP and good synergistic

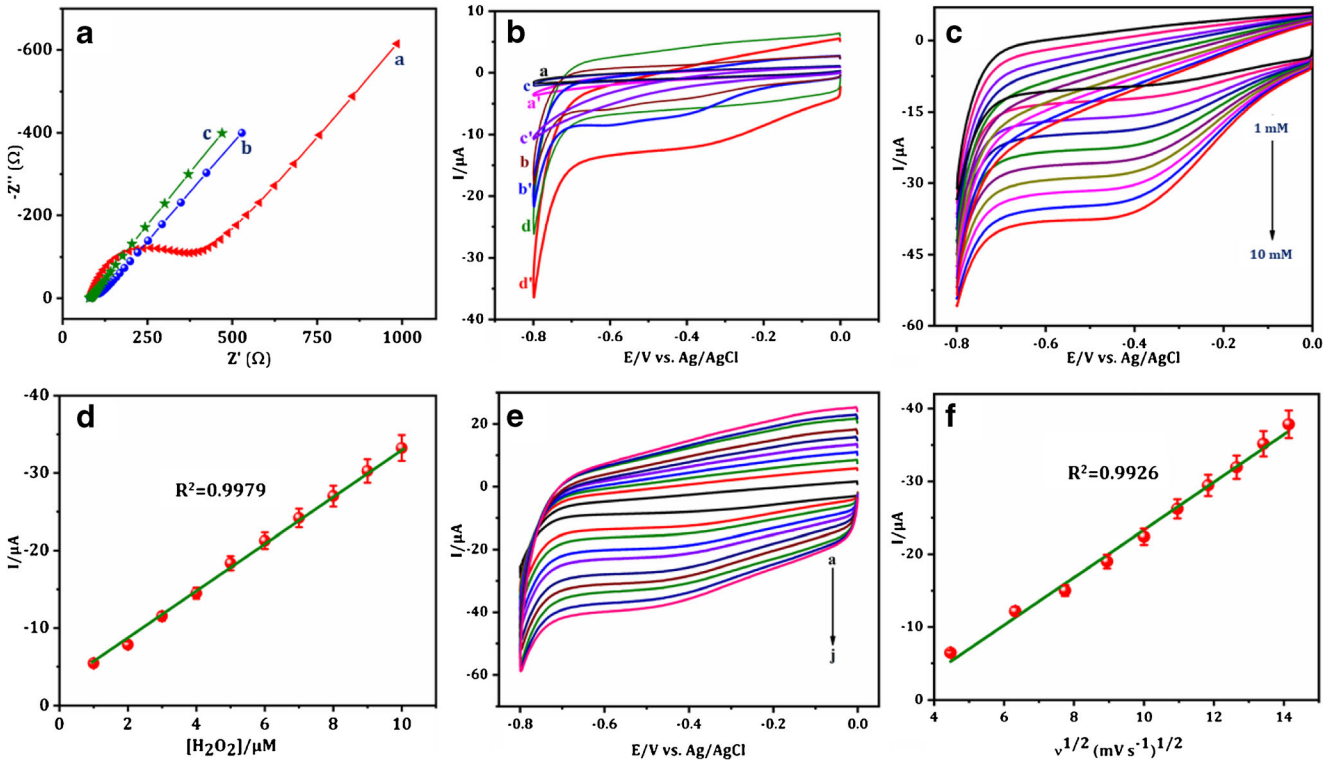

Fig. 3 **a** EIS of bare GCE (a), WC (b), and WCC (c). **b** CVs of bare GCE, WC/GCE, Co NP/GCE and WCC/GCE in the absence (a, b, c and d) and presence (a', b', c' and d') of 1 M H_2O_2 in 0.05 M phosphate buffer at a scan rate of 50 mV s^{-1}. **c** CVs of WCC/GCE in the presence of various concentration of H_2O_2 (1 to 10 mM) in 0.05 M phosphate buffer at a scan rate of 50 mV s^{-1}. **d** calibration plot between the cathodic current (Ipc) and $[H_2O_2]$ ($n = 3$). **e** CVs of WCC/GCE for 1 mM H_2O_2 in 0.05 M phosphate buffer at various scan rate. **f** calibration plot between the cathodic current (Ipc) and scan rates (n = 3)

effect can effectively enhanced the electrocatalytic reduction of H_2O_2; (ii) the high surface to volume ratio of the WC on the good conducting ability of Co nanoparticle boosted the catalytic efficiency; and (iii) the carried WC with Co nanoparticle might help as an intervening spacer matrix to extend the electron away from the substrate into the mobile phase, causing in binding sites more available to electron.

The influence of H_2O_2 concentration toward the electrocatalytic activities of WCC/GCE was scrutinized at different concentrations in N_2 saturated 0.05 M phosphate buffer at a scan rate of 50 mV s^{-1}. As shown Fig. 3c, upon increasing the concentration of H_2O_2 (1 to 10 mM), leads to the reduction current at −0.4 V (vs. Ag/AgCl) was gradually improved due to the strong catalytic reduction of H_2O_2. As we can see from Fig. 3d, the linearity was obtained between the reduction peak current and various concentration in the range of 1 to 10 mM with a correlation coefficient ($R^2 = 0.9979$).

The electro kinetics of H_2O_2 reduction at WCC/GCE was studied by analyzing the voltammograms at the scan rate range of 20–200 mV s^{-1} using 1 mM H_2O_2 in 0.05 M phosphate buffer (pH 7). As depicted in Fig. 3e, the obtained cathodic peak current (I_{pc}) were consecutively increased with an increase of scan rate from 20 to 200 mV s^{-1} (a-j). Moreover, the observed I_{pc} values were linearly correlated with the square root of the scan rate with a high correlation coefficient ($R^2 = 0.9926$), shown in Fig. 3f. Hence, it is clear that the electrochemical reduction of H_2O_2 at WCC/GCE unveiled diffusion-controlled process [12].

Amperometric studies

The quantitative detection of non-enzymatic H_2O_2 sensing properties of WCC was performed via amperometric i-t method. To find the optimal potential for H_2O_2 sensor, the amperometric measurements were carried out by applying various potentials including −0.2, −0.3, −0.4, −0.5, and − 0.6 V with the consecutive addition 100 μM H_2O_2 on WCC modified electrode. From Fig. 4a, the current response was obviously increased from −0.2 to −0.4 V and then decreased with further increase of operational potential (−0.5 and − 0.6 V) toward H_2O_2 detection. The current response reaches the highest value at −0.4 V and it was selected as an optimum potential for amperometric determination of non-enzymatic H_2O_2 sensor.

Figure 4b reveals the amperometric current response of WCC modified electrode on the successive addition of H_2O_2 concentration at an applied potential −0.4 V in to the N_2 saturated 0.05 M phosphate buffer (pH 7). As depicted in Fig. 4b, the responses toward H_2O_2 lead to swiftly, and a current response was accomplished with in a 5 s, due to H_2O_2 was quickly absorbed and activated on the WCC modified electrode surface. With consecutive addition of H_2O_2, the steady-

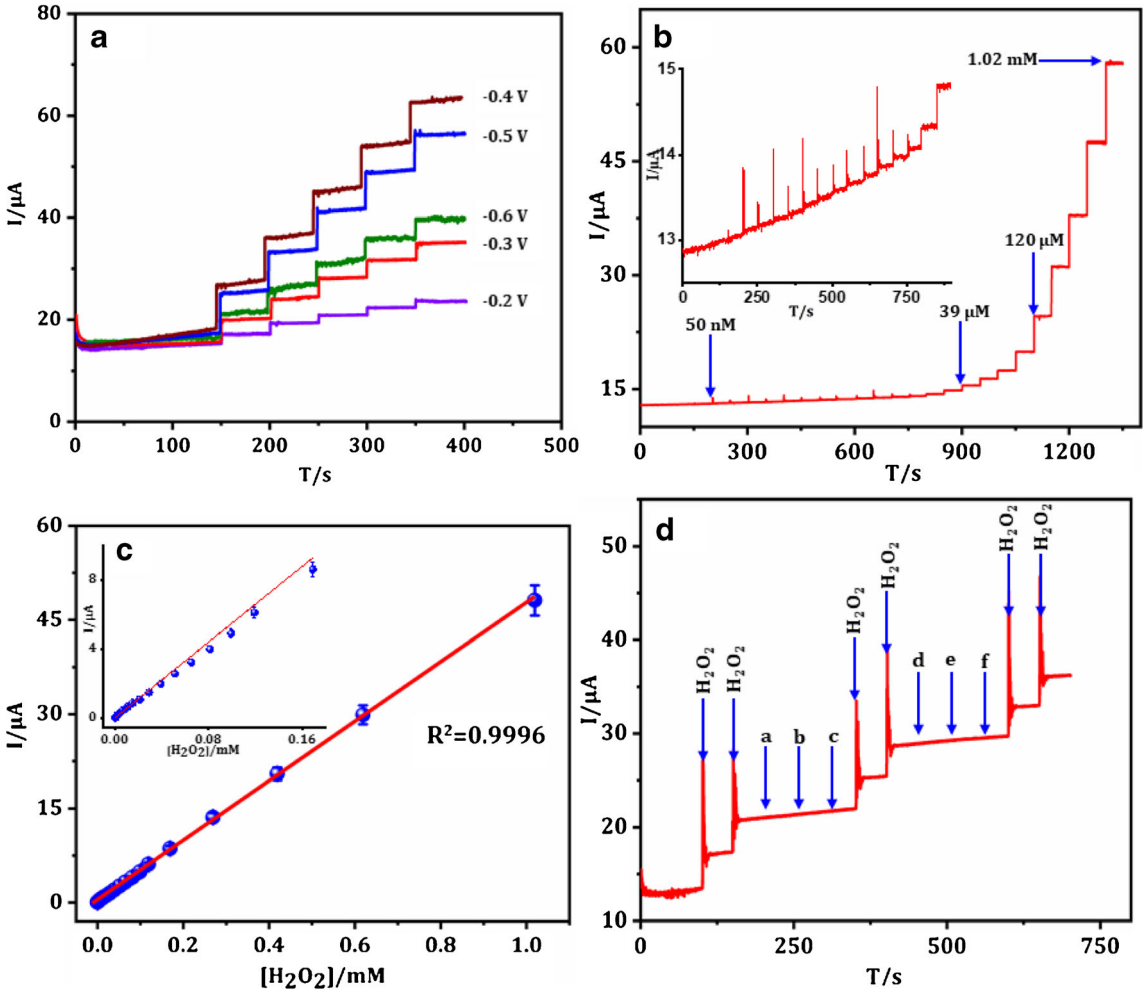

Fig. 4 **a** Amperometric current response of WCC modified electrode for consecutive addition of 100 μM H_2O_2 at different applied potential (−0.2, −0.3, −0.4, −0.5, and − 0.6 V). **b** Amperometric current response of WCC modified electrode for consecutive injection of various concentration of H_2O_2 at an applied potential of −0.4 V. **c** calibration plot between the response current and $[H_2O_2]$ ($n = 3$). **d** Amperometric current response of WCC modified electrode for 100 μM H_2O_2 and interferents (10-fold) such as dopamine (a), ascorbic acid (b), uric acid (c), glucose (d), albumin (e), and globulins (f) at an applied potential of −0.4 V

state reduction current increased progressively with increasing the concentration of H_2O_2 in the range from 50 nM to 1.02 mM. The corresponding correlation plots of H_2O_2 concentrations vs response current is manifested in Fig. 4c. This result demonstrates that the current and concentration of WCC establish a good linear relationship in the wide range 50 nM to 1.02 mM, correlation coefficient (R^2) is about 0.9996. The calculated detection limit and sensitivity of WCC modified electrode are to be 6.3 nM (signal to noise ratio $S/N = 3$) and 6.696 μA μM^{-1} cm^{-2}, respectively. Further, to elucidate the advantages of the sensor, the analytical parameters such as linear range, limit of detection for WCC modified electrode were compared with other reported non-enzymatic H_2O_2 sensor is displayed in Table 1. This results clearly proved WCC modified electrode has higher electro catalytic property and much better than those reported sensors with the perspectives of wide linear range and low detection limit.

Selectivity, stability, and reproducibility of the sensor

The most important features for a detection of H_2O_2 is the capability to distinguish amongst the target analyte and other possible interfering compounds. So as to evaluate the selectivity of the WCC modified electrode toward H_2O_2 was studied in the presence (5-fold) of co-interfering compounds such as dopamine (a), ascorbic acid (b), uric acid (c), glucose (d), albumin (e), and globulins (f) were carried out in 0.05 M phosphate buffer (pH 7) at a fixed potential of −0.4 V. Though, the aforementioned compounds were less answerable in the reduction potential. Figure 4d represents the amperometric i-t responses of 0.5 mM H_2O_2 with consecutive addition of aforementioned biologically active species. It can be seen that there is no remarkable response current was obtained upon addition of aforesaid interferents and they do not interfere with the reduction current response of H_2O_2. Besides a stable and well-defined current response was appeared for the further addition

Table. 1 Comparison of analytical parameters of WCC modified electrode with several reported non-enzymatic H_2O_2 sensors

Electrode	Linear range (mM)	LOD (μM)	Ref
BM NFs/Nf/GCE	0.0002–0.29	0.05	[2]
Nf/Gr-CCS/AgNPs/GCE	0.02–5.02	2.49	[4]
$CoFe_2O_4$ HS/GCE	0.01–1.2	2.5	[5]
GNPs/GN-CS/GCE	0.005–35	0.0016	[6]
Ag/boehmite nanotubes/rGO/GCE	0.0005–10	0.17	[11]
rGO/Ag/PdNPs/GCE	0.005–14.65	1.1	[15]
N-GrNRs	0.005–0.085, 0.135–1.285	1.72	[16]
CuO@Cu_2O–NWs/PVA	0.001–3	0.35	[17]
Cu_2O/PANI/rGO/GCE	0.0008–12.78	0.5	[34]
3D GOx/PB/NGFE	0.2–20.0	100	[35]
WC-Co NP/GCE	50 nM to 1.02 mM	0.0063	This work

BM NFs-Bi_2O_3/MnO_2 nanoflowers; Nf-Nafion; rGO-reduced graphene oxide; Pd NPs-palladium nanoparticles; Ag NPs-silver nanoparticles; Gr-CCS- graphene-colloidal carbon sphere; MC –mesoporous carbon; GS-graphene sheets; GE-gold electrode; CPE-carbon paste electrode; CQDs-carbon quantum dots; Pt-platinum; Cu-copper; PSi-silicon powder; CILE-carbon ionic liquid electrode

of H_2O_2. These results established that WCC modified electrode can be selectively determined the H_2O_2 even in the presence of aforementioned interfering compounds.

To evaluate the stability of the sensor, the modified electrode was stored at room temperature for 30 days and the reduction current response toward 1 μM H_2O_2 was examined every five days. The sensor kept 95.6% of its initial current responses at 30th day, suggesting a good stability. The reproducibility of the WCC modified electrode was studied toward the detection of H_2O_2 sensor. The sensor exhibited a relative standard deviation (RSD) of about 2.09% for the 1 μM H_2O_2 detection with ten consecutive measurements under the same condition. These results indicate that the WCC modified electrode has good reproducibility.

Table 2 Detection of H_2O_2 in commercial contact lens solution and human blood serum samples by WCC modified electrode

Sample	Spiked (μM)	Found (μM)	Recovery (%)	RSD (%) (n = 3)
Contact lens solution	5.0	4.96	99.2	2.01
	10.0	9.94	99.4	1.97
	15.0	14.9	99.3	1.84
Human blood serum	5.0	4.93	98.6	2.15
	10.0	9.95	99.5	2.07
	15.0	14.89	99.26	1.95

Real sample analysis

To assess the feasibility of WCC modified electrode for practical analysis, the sensor was applied to determine the H_2O_2 content in lens-cleaning solution and human blood serum samples with standard addition method. The samples were spiked and diluted through the N_2-saturated 0.05 M phosphate buffer (pH 7) prior to determine the response current. Then, the current response was analyzed after adding the standard H_2O_2 solution into the system. The obtained recoveries for contact lens solution and human blood serum samples is about 99.3% and 99.12%, respectively (Table 2). The satisfactory recoveries are demonstrated that the sensor has good accuracy in the detection of H_2O_2 in real time applications.

Conclusion

A simple synthesis method for the cobalt nanoparticle anchored tungsten carbide (WC) flakes with excellent catalytic activity for non-enzymatic detection of H_2O_2 is reported. The decoration of cobalt nanoparticles significantly accelerated the electron conducting ability of the WCC, creates synergistic effects and thus making this highly effective candidate to detect H_2O_2. The amperometric responses of WCC improved sensing performance with a detection limit of 6.3 nM, wide linear range of 50 nM-1.02 mM and rapid response time (5 s) toward H_2O_2. Owing to the enhanced catalytic activity, WCC showed excellent selectivity, stability and reproducibility. In real sample analysis, the sensor was achieved the good accuracy and high precision for H_2O_2 detection in contact lens solution and human blood serum samples. Hence, this method was easy way to create high efficiency non-enzymatic H_2O_2 sensor.

Acknowledgements The authors gratefully acknowledge the financial support of the Ministry of Science and Technology, Taiwan through contract no. MOST 107-2113-M-027-005-MY3.

Compliance with ethical standards The author(s) declare that they have no competing interests.

References

1. Xie F, Cao X, Qu F, Asiri AM, Sun X (2018) Cobalt nitride nanowire array as an efficient electrochemical sensor for glucose and H_2O_2 detection. Sensors Actuators B Chem 255:1254–1261
2. Ray C, Dutta S, Roy A, Sahoo R, Pal T (2016) Redox mediated synthesis of hierarchical Bi_2O_3/MnO_2 nanoflowers: a non-enzymatic hydrogen peroxide electrochemical sensor. Dalton Trans 45:4780–4790
3. Chen W, Cai S, Ren QQ, Wen W, Zhao YD (2012) Recent advances in electrochemical sensing for hydrogen peroxide: a review. Analyst 137:49–58
4. Wang H, Wang H, Li T, Ma J, Li K, Zuo X (2017) Silver nanoparticles selectively deposited on graphene-colloidal carbon sphere

composites and their application for hydrogen peroxide sensing. Sensors Actuators B Chem 239:1205–1212
5. Vasuki K, Babu KJ, Sheet S, Siva G, Kim AR, Yoo DJ (2017) Amperometric hydrogen peroxide sensor based on the use of $CoFe_2O_4$ hollow nanostructures. Microchim Acta 184:2579–2586
6. Jia N, Huang B, Chen L, Tan L, Yao S (2014) A simple non-enzymatic hydrogen peroxide sensor using gold nanoparticles-graphene-chitosan modified electrode. Sensors Actuators B Chem 195:165–170
7. Kim JH, Patra CR, Arkalgud JR, Boghossian AA, Zhang J, Han JH, Reuel NF, Ahn JH, Mukhopadhyay D, Strano MS (2011) Single-molecule detection of H_2O_2 mediating angiogenic redox signaling on fluorescent single-walled carbon nanotube array. ACS Nano 5: 7848–7857
8. Yue HF, Bu X, Huang MH, Young J, Raglione T (2009) Quantitative determination of trace levels of hydrogen peroxide in crospovidone and a pharmaceutical product using high performance liquid chromatography with coulometric detection. Int J Pharm 375:33–40
9. Matsubara C, Kawamoto N, Takamura K (1992) Oxo [5, 10, 15, 20-tetra (4-pyridyl) porphyrinato] titanium (IV): an ultra-high sensitivity spectrophotometric reagent for hydrogen peroxide. Analyst 117:1781–1784
10. Hanaoka S, Lin JM, Yamada M (2001) Chemiluminescent flow sensor for H_2O_2 based on the decomposition of H_2O_2 catalyzed by cobalt (II)-ethanolamine complex immobilized on resin. Anal Chim Acta 426:57–64
11. Zhao C, Zhang H, Zheng J (2017) A non-enzymatic electrochemical hydrogen peroxide sensor based on ag decorated boehmite nanotubes/reduced graphene oxide nanocomposites. J Electroanal Chem 784:55–61
12. Liu H, Weng L, Yang C (2017) A review on nanomaterial-based electrochemical sensors for H_2O_2, H_2S and NO inside cells or released by cells. Microchim Acta 184:1267–1283
13. Liu W, Zhou Z, Yin L, Zhu Y, Zhao J, Zhu B, Zheng L, Jin Q, Wang L (2018) A novel self-powered bioelectrochemical sensor based on $CoMn_2O_4$ nanoparticle modified cathode for sensitive and rapid detection of hydrogen peroxide. Sensors Actuators B Chem 271: 247–255
14. Balasubramanian P, Annalakshmi M, Chen SM, Sathesh T, Peng TK, Balamurugan TST (2018) Facile solvothermal preparation of Mn_2CuO_4 microspheres: excellent electrocatalyst for real-time detection of H_2O_2 released from live cells. ACS Appl Mater Interfaces 10:43543–43551
15. Amala G, Saravanan J, Yoo DJ, Kim AR (2017) An environmentally benign one pot green synthesis of reduced graphene oxide-based composites for the enzyme free electrochemical detection of hydrogen peroxide. New J Chem 41:4022–4030
16. Shi LB, Niu XH, Liu TT, Zhao HL, Lan MB (2015) Electrocatalytic sensing of hydrogen peroxide using a screen-printed carbon electrode modified with nitrogen-doped graphene nanoribbons. Microchim Acta 68:358–364
17. Chirizzi D, Guascito MR, Filippo E, Malitesta C, Tepore A (2016) A novel nonenzymatic amperometric hydrogen peroxide sensor based on CuO@Cu_2O nanowires embedded into poly(vinyl alcohol). Talanta 147:124–131
18. Morishita T, Soneda Y, Hatori H, Inagaki M (2007) Carbon-coated tungsten and molybdenum carbides for electrode of electrochemical capacitor. Electrochim Acta 52:2478–2484
19. Guo Q, Liang F, Gao XY, Gan QC, Li XB, Li J, Lin Z, Tung CH, Wu LZ (2018) Metallic Co_2C: a promising Cocatalyst to boost photocatalytic hydrogen evolution of colloidal quantum dots. ACS Catal 8:5890–5895
20. Chhina H, Campbell S, Kesler O (2007) Ex situ evaluation of tungsten oxide as a catalyst support for PEMFCs. J Electrochem Soc 154:B533–B539
21. Li S, Yang C, Yin Z, Yang H, Chen Y, Lin L, Li M, Li W, Hu G, Ma D (2017) Wet-chemistry synthesis of cobalt carbide nanoparticles as highly active and stable Electrocatalyst for hydrogen evolution reaction. Nano Res 10:1322–1328
22. Fan HS, Yu H, Zhang Y, Zheng Y, Luo Y, Dai Z, Li B, Zong Y, Yan QY (2017) Fe doped Ni_3C Nanodots in N-doped carbon Nanosheets for efficient hydrogen-evolution and oxygen-evolution Electrocatalyst. Angew Chem Int Ed 56:12566–12570
23. Meyer S, Nikiforov AV, Petrushina IM, Köhler K, Christensen E, Jensen JO, Bjerrum NJ (2015) Transition metal carbides (WC, Mo_2C, TaC, NbC) as potential electrocatalysts for the hydrogen evolution reaction (HER) at medium temperatures. Int J Hydrog Energy 40:2905–2911
24. Burakov VS, Butsen AV, Brüser V, Harnisch F, Misakov PY, Nevar EA, Rosenbaum M, Savastenko NA, Tarasenko NV (2008) Synthesis of tungsten carbide nanopowder via submerged discharge method. J Nanopart Res 10:881–886
25. Liu C, Zhou J, Xiao Y, Yang L, Yang D, Zhou D (2017) Structural and electrochemical studies of tungsten carbide/carbon composites for hydrogen evolution. Int J Hydrog Energy 42:29781–29790
26. Xu YT, Xiao X, Ye ZM, Zhao S, Shen R, He CT, Chen XM (2017) Cage-confinement pyrolysis route to ultrasmall tungsten carbide nanoparticles for efficient electrocatalytic hydrogen evolution. J Am Chem Soc 139:5285–5288
27. Zeng M, Chen Y, Li J, Xue H, Mendes RG, Liu J, Zhang T, Ruemmeli MH, Fu L (2017) 2D WC single crystal embedded in graphene for enhancing hydrogen evolution reaction. Nano Energy 33:356–362
28. Lin H, Liu N, Shi Z, Guo Y, Tang Y, Gao Q (2016) Cobalt-doping in molybdenum-carbide nanowires toward efficient electrocatalytic hydrogen evolution. Adv Funct Mater 26:5590–5598
29. Tominaga H, Aoki Y, Nagai M (2012) Hydrogenation of CO on molybdenum and cobalt molybdenum carbides. Appl Catal A Gen 423:192–204
30. Gao Q, Zhang W, Shi Z, Yang L, Tang Y (2018) Structural design and electronic modulation of transition-metal-carbide Electrocatalysts toward efficient hydrogen evolution. Adv Mater 31:1802880. https://doi.org/10.1002/adma.201802880
31. Xu YT, Xiao X, Ye ZM, Zhao S, Shen R, He CT, Zhang JP, Li Y, Chen XM (2017) Cage-confinement pyrolysis route to ultrasmall tungsten carbide nanoparticles for efficient electrocatalytic hydrogen evolution. J Am Chem Soc 139:5285–5288
32. Wu HX, Zhang CX, Jin L, Yang H, Yang SP (2010) Preparation and magnetic properties of cobalt nanoparticles with dendrimers as templates. Mater Chem Phys 121:342–348
33. Srinivas K, Vithal M, Sreedhar B, Raja MM, Reddy PV (2009) Structural, optical, and magnetic properties of Nanocrystalline co doped SnO_2 based diluted magnetic semiconductors. J Phys Chem C 113:3543–3552
34. Liu J, Yang C, Shang Y, Zhang P, Liu J, Zheng J (2018) Preparation of a nanocomposite material consisting of cuprous oxide, polyaniline and reduced graphene oxide, and its application to the electrochemical determination of hydrogen peroxide. Microchim Acta 185:172
35. Zhang Y, Huang B, Yu F, Yuan Q, Gu M, Ji J, Li Y (2018) 3D nitrogen-doped graphite foam@Prussian blue: an electrochemical sensing platform for highly sensitive determination of H_2O_2 and glucose. Microchim Acta 185:86